NJC

PAPER

View Article Online
View Journal | View Issue

Cite this: *New J. Chem.*, 2015, **39**, 7429

Probing the effect of arm length and inter- and intramolecular interactions in the formation of Cu(II) complexes of Schiff base ligands derived from some unsymmetrical tripodal amines†

Hassan Keypour,*[a] Maryam Shayesteh,[a] Sadegh Salehzadeh,[a] Sébastien Dhers,[b] Farahnaz Maleki,[a] Hüseyin Ünver[c] and Nefise Dilek[d]

Received (in Victoria, Australia) 25th May 2015,
Accepted 20th July 2015

DOI: 10.1039/c5nj01318f

www.rsc.org/njc

The syntheses of two previously known, 2-((2-aminoethyl)(pyridin-2-ylmethyl)amino)ethanol (**1**) and 2-((3-aminopropyl)(pyridin-2-ylmethyl)amino)ethanol (**2**), and four new unsymmetrical N-capped tripodal amines, 2-((4-aminobutyl)(pyridin-2-ylmethyl)amino)ethanol (**3**), 3-((2-aminoethyl)(pyridin-2-ylmethyl)amino)-propan-1-ol (**4**), 3-((3-aminopropyl)(pyridin-2-ylmethyl)amino)propan-1-ol (**5**) and 3-((4-aminobutyl)(pyridin-2-ylmethyl)amino)propan-1-ol (**6**), are reported. The ligands (**3–4**) feature a longer arm, 3-hydroxypropyl or butylamino, than in the analogues previously employed (2-hydroxyethyl arm, ethylamino-arm or propylamino-arm in **1** and **2**). All six tripodal amines, **1–6**, are equipped with a 2-methylpyridyl-arm and either an ethylamino-arm (**1** and **4**), propylamino-arm (**2** and **5**) or butylamino-arm (**3** and **6**). The new amines, **3–6**, have been employed in one pot condensation reactions with 2-hydroxy-1-naphthaldehyde and salicylaldehyde (and its derivatives) in the presence of Cu(II) metal ions to generate a series of new mononuclear complexes, $[M^{II}\mathbf{L}^{aldi}](ClO_4)$ as well as new dinuclear complexes $[Cu^{II}\mathbf{L}^{aldi}]_2(ClO_4)_2$ of new ligands $\mathbf{L}^{aldi}$. Four monomeric complexes and one dimeric complex have been characterised by single crystal X-ray diffraction, revealing a distorted square-pyramidal copper(II) ion. A general comparison between these structures shows that the number and types of chelate ring sequences around the metal ions are important in the formation of structures. Theoretical studies show that the 3-hydroxypropyl arm in these complexes is a weak coordinating group and it can readily be removed from the coordination sphere of metal ions, resulting in a dimerised four coordinate complex. Calculations show that the interaction between the two monomeric fragments is very weak.

Introduction

Recently, research on tripodal ligands and their related complexes has been an expanding field and is the subject of numerous reports.[1] Transition metal complexes synthesised with this type of ligand display special physical, chemical or structural properties, such as unusual conformation, high thermodynamic stability and virtual kinetic inertness.[2] These tripodal ligands can also serve as precursors for the synthesis of interesting macrobicyclic compounds[3,4] which usually requires high dilution techniques[5] or the use of metal ions as templates.[6,7] The synthesis of model complexes mimicking the spectroscopic and structural properties of metalloprotein active sites can be undertaken by employing multidentate tripodal ligands, most of which possess aromatic donor functions like pyridyl and/or phenolic groups.[8] However, the chemistry of asymmetric N-capped tripodal ligands which possess three pendant arms with different donor groups has not been well explored.[9,10] This type of tripodal ligand is of particular interest in the context of modeling the asymmetric active metal sites such as those found in nitrile hydratase[11] and horse liver alcohol dehydrogenase.[12] Among these asymmetric N-capped tripodal ligands, our group is particularly interested in unsymmetric N-capped tripodal ligands with two different aliphatic arm lengths and one aromatic pendant arm. However these tripodal

[a] *Faculty of Chemistry, Bu-Ali Sina University, Hamedan 65174, Iran. E-mail: haskey1@yahoo.com; Fax: +98 8118 380709; Tel: +98 9188131117*
[b] *Department of Chemistry and The MacDiarmid Institute for Advanced Materials and Nanotechnology, University of Otago, P. O. Box 56, Dunedin 9054, New Zealand*
[c] *Department of Physics, Faculty of Science, Ankara University, TR-06100 Tandogan, Ankara, Turkey*
[d] *Department of Physics, Arts and Sciences Faculty, Aksaray University, TR-68100, Aksaray, Turkey*

† Electronic supplementary information (ESI) available: ^{1}H NMR, ^{13}C NMR and IR spectra of amines (**3–6**) (Fig. S1–S12), IR spectra of complexes (Fig. S13–S30), and mass spectra of complexes (Fig. S31–S48). CCDC 968863 $[Cu^{II}\mathbf{L}^{napht2}](ClO_4)$, 968865 $[Cu^{II}\mathbf{L}^{H3}](ClO_4)$, 1002225 $[Cu^{II}\mathbf{L}^{OMe3}](ClO_4)$, 1002229 $[Cu^{II}\mathbf{L}^{H4}](ClO_4)$ and 1002230 $[Cu^{II}\mathbf{L}^{H5}]_2(ClO_4)_2$. For ESI and crystallographic data in CIF or other electronic format see DOI: 10.1039/c5nj01318f

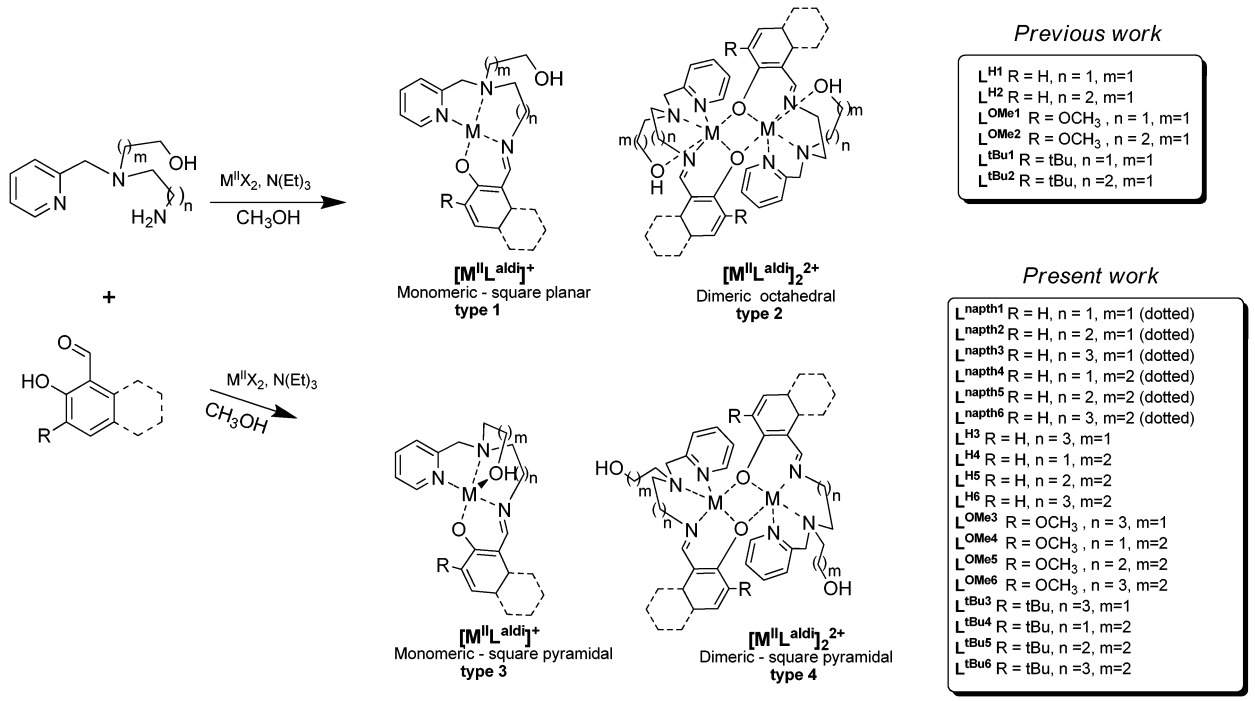

Fig. 1 Summary of the range of structural motifs identified to date for complexes resulting from the condensation of a range of salicylaldehydes with the unsymmetrical triamines 1 (n = 1 and m = 1) and 2 (n = 2 and m = 1) with 2-hydroxyethyl arms but differing amino-arm lengths. The present study concerns complexes of the new ligands highlighted in the box, HL^{H3-6}, HL^{OMe3-6}, HL^{tBu3-6} and $HL^{napht1-6}$ (X = ClO_4^-).

ligands bearing one pyridine arm are scarce.[13] As part of a program to explore the coordination chemistry of partially unsymmetric tripodal N_3O_2 ligands, we herein report the synthesis and characterisation of new Cu complexes and compare them with our previous work. A direct influence of the lengths of the alkyl chains between central and terminal donor functions on the complex geometry was observed for the cadmium(II), nickel(II) and copper(II) complexes of these unsymmetrical tripodal ligands featuring different spacer lengths (Fig. 1). The coordination behavior towards Cd(II), Ni(II) and Cu(II) was investigated for ligands L^{aldi} combining pyridine, amine, and alkoxy donor functions on ethylene, propylene and butylene spacers.[14]

In previous work, we reported the synthesis of two new unsymmetrical triamines, **1** and **2**, both of which feature three different arms: 2-methylpyridyl, either ethylamino- or propylamino, and ethanol (Fig. 1).[14] Reaction of **1** or **2** with salicylaldehyde and its analogues gave a wide selection of compounds with which to probe the effects of strain in the resulting cadmium(II) and nickel(II) Schiff base complexes (Fig. 1).[14] When the shorter ethylene linker was used between the tertiary and primary amine nitrogen atoms, a mononuclear Schiff base complex was structurally characterised in the case of $[Ni^{II}L^{OMe1}]^+$ whereas the more flexible propylene linker (L^{OMe2} and L^{H2} ligands) gave dinuclear complexes, $[Ni^{II}L^{OMe2}]_2^{2+}$ and $[Cd^{II}L^{H2}]_2^{2+}$, which were structurally characterised. The nickel(II) centre in $[Ni^{II}L^{OMe1}]^+$ has a distorted square planar geometry, whereas in $[Ni^{II}L^{OMe2}]_2^{2+}$ the geometry is distorted octahedral, as with the cadmium(II) ion in $[Cd^{II}L^{H2}]_2^{2+}$.[14] The structural types observed to date are summarised in Fig. 1.

In this paper the effect of employing a 3-hydroxypropyl arm in place of the 2-hydroxyethyl arm, and a butylamino arm in place of the ethylamino or propylamino arm on the outcome of one pot condensations with various salicylaldehydes in the presence of copper(II) ions has been studied. Hence the synthesis of four new unsymmetrical tripodal triamines, 2-((4-aminobutyl)-(pyridin-2-ylmethyl)amino)ethanol (**3**), 3-((2-aminoethyl)(pyridin-2-ylmethyl)amino)propan-1-ol (**4**), 3-((3-aminopropyl)(pyridin-2-ylmethyl)amino)propan-1-ol (**5**) or 3-((4-aminobutyl)(pyridin-2-ylmethyl)amino)propan-1-ol (**6**), is reported (Fig. 1). The synthesis and physical properties of the new Cu(II) complexes of the new ligands, HL^{H3-6}, HL^{OMe3-6} and HL^{tBu3-6} formed *in situ* from the condensation of 2-hydroxybenzaldehyde with **3–6** (HL^{H3-6}), 2-hydroxy-3-methoxy-benzaldehyde with **3–6** (HL^{OMe3-6}), 3,5-di-*tert*-butylsalicylaldehyde with **3–6** (HL^{tBu3-6}) and, for the first time, 2-hydroxy-1-naphthaldehyde with **1–6** ($HL^{napht1-6}$), are reported here. In addition, the X-ray crystal structures of $[Cu^{II}L^{napht2}](ClO_4)$, $[Cu^{II}L^{OMe3}](ClO_4)$, $[Cu^{II}L^{H3}](ClO_4)$, $[Cu^{II}L^{H4}](ClO_4)$ and dimeric $[Cu^{II}L^{H5}]_2(ClO_4)_2$ are described.

Results and discussion

Four new unsymmetrical tripodal amines, 2-((4-aminobutyl)-(pyridin-2-ylmethyl)amino)ethanol (**3**), 3-((2-aminoethyl)(pyridin-2-ylmethyl)amino)propan-1-ol (**4**), 3-((3-aminopropyl)(pyridin-2-ylmethyl)amino)propan-1-ol (**5**) and 3-((4-aminobutyl)(pyridin-2-ylmethyl)amino)propan-1-ol (**6**), were prepared in high yields. Amines **3–6** differ from the previously used amines, **1** and **2**, in

that **4** and **5** feature a 3-hydroxypropyl arm in place of the 2-hydroxyethyl arm, **3** features a butylamino arm in place of the ethylamino/propylamino arm and **6** features a 3-hydroxypropyl arm in place of the 2-hydroxyethyl arm and also a butylamino arm in place of the ethylamino/propylamino arm (Fig. S1–S12, ESI†). Subsequently, one pot reactions of amines **1–6** with 2-hydroxy-1-naphthaldehyde and salicylaldehyde derivatives in the presence of a Cu(II) metal salt were employed to generate new Cu(II) complexes of Schiff-base ligands $\mathbf{L^{aldi}}$, where **aldi** is **H3–6**, **OMe3–6**, ***t*Bu3–6** and **napht1–6** (Fig. 1). Recrystallisation of powders obtained from the reaction mixture by vapour diffusion of diethyl ether (see the Experimental section below) gave either purified powders or single crystals which were analysed by single crystal X-ray diffraction, showing four monomeric and one dimeric compounds (*vide infra*).

The infrared spectra of all complexes (Fig. S13–S30, ESI†) show a band at *ca.* 1613–1632 cm^{-1}, attributable to the imine groups, and no bands due to ν(C=O) vibrations. Medium to strong bands at *ca.* 1596–1612 and 1437–1462 cm^{-1} are present in all cases, and correspond to the two highest energy ring vibrations of the coordinated pyridine.[14,15] Absorptions attributable to the perchlorate ions are seen at approximately 1051–1088 and 619–625 cm^{-1}. The lack of splitting suggests that they are not coordinated.

The positive ion electrospray mass spectra of all complexes (Fig. S31–S48, ESI†) show a common peak, which is the fragment $[Cu^{II}\mathbf{L^{aldi}}]^+$ associated with the loss of the ClO_4^- anion. The four copper(II) complexes using $(\mathbf{L^{ald5}})^-$ as a ligand appear to be dimeric complexes $[Cu^{II}\mathbf{L^{ald5}}]_2(ClO_4)_2$ as the mass spectra exhibit peaks of very weak intensity consistent with the presence of a dication $[Cu\mathbf{L^{ald5}}]_2^{2+}$. In all copper(II) complexes the most intense peaks are for the mononuclear $[Cu^{II}\mathbf{L^{aldi}}]^+$ species which indicates that the dimer is unsurprisingly broken apart. On the other hand, a peak with a very weak intensity corresponding to the $[M\mathbf{L^{aldi}}]_2^+$ fragment is observed in most of the mononuclear complexes in present work and also in our previous work,[14] even when their X-ray crystal structures show that they are mononuclear complexes. Thus it seems that the $[M\mathbf{L^{aldi}}]_2^+$ fragment observed in the mass spectra of the mononuclear complexes is formed due to a very small dimerization occurring in the mass spectrometer.

UV-Vis spectra of the fourtheen Cu(II) complexes in CH_3CN solution showed a broad low-intensity absorption band occurring in the range 574 nm $< \lambda_{max} <$ 630 nm with molar extinction coefficient ranging between 92 M^{-1} cm^{-1} $< \varepsilon <$ 174 M^{-1} cm^{-1}. This is assigned to a d–d transition and is characteristic of five-coordinate copper(II) complexes with square pyramidal or distorted square pyramidal geometries, which generally exhibit a band in the 550–660 nm range (d_{xz}, $d_{yz} \rightarrow d_{x^2-y^2}$).[16–24] In the case of four Cu complexes $[Cu^{II}\mathbf{L^{aldi}}]$-$ClO_4$ (i = 3), the respective λ_{max} values in the range 600 nm $< \lambda_{max} <$ 633 nm and 121 M^{-1} cm^{-1} $< \varepsilon <$ 157 M^{-1} cm^{-1} (each with a shoulder at 761–819 nm) are also indicative of square-pyramidal coordination according to the literature.[25,26] In addition, a few absorption bands are found in the range 205–406 nm for all Cu(II) complexes, due to either charge transfer or π–π* transitions.[19,21,27–29] Although the UV-Vis spectra of complexes with polydentate Schiff base ligands are not generally good indicators of geometry, the evidence gathered helps to support this geometry.

Room temperature magnetic moments were obtained for all mononuclear Cu(II) complexes. The magnetic moment values for these complexes lie in the 1.82–1.95 BM range. These values are close to the expected spin only magnetic moment value (1.73 BM) for the d^9 Cu(II) system[30] with single unpaired electron. For the four dinuclear copper complexes, the observed values of magnetic moment lie in the 1.32–1.66 BM range per Cu atom.

Crystal structures of $[Cu^{II}\mathbf{L^{napht2}}](ClO_4)$, $[Cu^{II}\mathbf{L^{H3}}](ClO_4)$, $[Cu^{II}\mathbf{L^{OMe3}}](ClO_4)$ and $[Cu^{II}\mathbf{L^{H4}}](ClO_4)$

Green single crystals of $[Cu^{II}\mathbf{L^{napht2}}](ClO_4)$, $[Cu^{II}\mathbf{L^{H3}}](ClO_4)$, $[Cu^{II}\mathbf{L^{OMe3}}](ClO_4)$ and $[Cu^{II}\mathbf{L^{H4}}](ClO_4)$ suitable to be studied by X-ray diffraction were obtained by slow diffusion of diethyl ether into a solution of the complex in MeOH. Crystal data and structure refinement are given in Table 1. These complexes are monometallic but differ in the space group adopted ($P2_1/c$, $C2/c$, $P\bar{1}$ and $I2/a$, respectively). The molecular structures as well as

Table 1 Crystal data and structure refinement parameters for $[Cu^{II}\mathbf{L^{napht2}}](ClO_4)$, $[Cu^{II}\mathbf{L^{H3}}](ClO_4)$, $[Cu^{II}\mathbf{L^{OMe3}}](ClO_4)$, $[Cu^{II}\mathbf{L^{H4}}](ClO_4)$ and $[Cu^{II}\mathbf{L^{H5}}]_2(ClO_4)_2$

Compound	$[Cu^{II}\mathbf{L^{napht2}}](ClO_4)$	$[Cu^{II}\mathbf{L^{H3}}](ClO_4)$	$[Cu^{II}\mathbf{L^{OMe3}}](ClO_4)$	$[Cu^{II}\mathbf{L^{H4}}](ClO_4)$	$[Cu^{II}\mathbf{L^{H5}}]_2(ClO_4)_2$
Formula	$C_{22}H_{24}ClCuN_3O_6$	$C_{19}H_{24}ClCuN_3O_6$	$C_{44}H_{62}Cl_2Cu_2N_6O_{15}$	$C_{18}H_{22}ClCuN_3O_6$	$C_{38}H_{48}Cl_2Cu_2N_6O_{12}$
Molecular weight (g mol^{-1})	525.43	488.39	1112.98	475.38	978.80
T (K)	100(2)	296	100(2)	89(2)	100(2)
Crystal system	Monoclinic	Monoclinic	Triclinic	Monoclinic	Orthorhombic
Space group	$P2_1/c$	$C2/c$	$P\bar{1}$	$I2/a$	$Pbca$
Z	4	8	4	8	4
a (Å)	13.1270(2)	11.5021(3)	13.9094(3)	19.0697(4)	12.2844(2)
b (Å)	13.7157(2)	18.7307(5)	18.2391(4)	10.6833(2)	14.1806(2)
c (Å)	12.1763(2)	20.7277(7)	20.6775(6)	18.9974(3)	23.1490(3)
α (°)	90	90	90.039(2)	90	90
β (°)	103.203(2)	95.504(1)	91.901(2)	95.766(2)	90
γ (°)	90	90	111.884(2)	90	90
V (Å^3)	2134.34(6)	4445.0(2)	4864.6(2)	3850.71(12)	4032.56(10)
Density (g cm^{-3})	1.635	1.460	1.520	1.640	1.612
R_1	0.0308	0.045	0.1565	0.0382	0.0878
wR_2	0.0809	0.138	0.3908	0.1218	0.2657

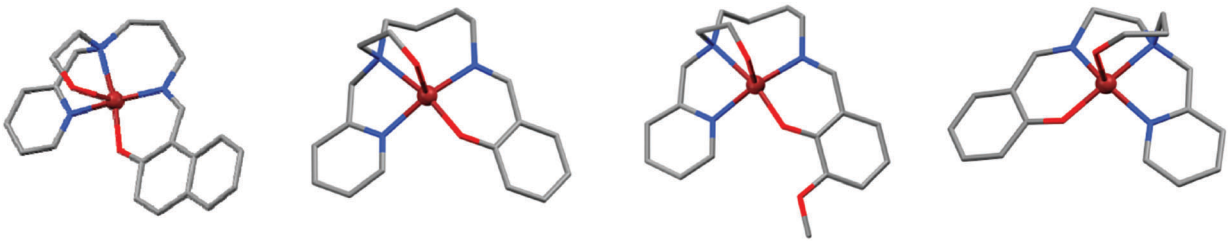

Fig. 2 Perspective of (from left to right) $[Cu^{II}L^{napht2}](ClO_4)$, $[Cu^{II}L^{H3}](ClO_4)$, $[Cu^{II}L^{OMe3}](ClO_4)$ and $[Cu^{II}L^{H4}](ClO_4)$. Hydrogen atoms and anions are omitted for clarity. Cu, C, N and O are represented in dark red, gray, blue and red, respectively.

selected bond lengths and angles are given in Fig. 2 and Table 2, respectively, and a comparison with the literature is also shown. The X-ray crystal structures of these complexes consist of $[Cu^{II}L^{napht2}]^+$, $[Cu^{II}L^{H3}]^+$, $[Cu^{II}L^{OMe3}]^+$ and $[Cu^{II}L^{H4}]^+$ cations and perchlorate anions. The Cu(II) ion displays a distorted square pyramidal coordination, involving three N atoms and two O atoms. In comparison to the mononuclear $[Ni^{II}L^{OMe1}](ClO_4)$ complex reported in our previous work,[14] in which the hydroxyl group is not coordinated, in these mononuclear copper(II) complexes it is coordinated to the apical site of the approximate square pyramidal copper(II) ion (Table 2). As expected, this axially bound O donor atom makes a bond that is slightly longer than bond distances in the basal plane ($\sim$2 Å). Among the Cu–N bonds, those involving the tertiary amine nitrogen atoms are the longest in all Cu complexes. The second longest Cu–N bond formed in both mononuclear and dinuclear complexes involves the Cu–N_{py} bonds. Comparison of the same bond lengths of square pyramidal Cu(II) complexes reported here with related reports in the literature is summarised in Table 2.[14,19,31–38]

The X-ray crystal structure analysis shows that in the case of $[Cu^{II}L^{OMe3}](ClO_4)$, two $[Cu^{II}L^{OMe3}]^+$ cations are bonded through hydrogen bonding. Indeed, the hydrogen atom of the hydroxyl group of one cation is engaged in hydrogen bonding with the phenolic oxygen atom of the adjacent cation and *vice versa* (Fig. 5a). It seems that these intermolecular interactions between two molecules of such five coordinate complexes in $[Cu^{II}L^{OMe3}](ClO_4)$ are relatively strong and prevent the formation of dinuclear compounds (see the Theoretical studies section). Note that the dataset for $[Cu^{II}L^{OMe3}](ClO_4)$ was particularly bad, leading to a high R_1 factor, this despite our best efforts to grow better crystals, the results presented here are from the best dataset obtained.

Variation of the length of the ligand arms leads to different sizes of chelate rings. These tripodal ligands are capable of forming both five and six membered chelate rings incorporating the copper ion in $[Cu^{II}L^{napht2}](ClO_4)$, $[Cu^{II}L^{H4}](ClO_4)$ and $[Cu^{II}L^{H5}]_2(ClO_4)_2$ and also five, six and seven membered chelate rings in $[Cu^{II}L^{H3}](ClO_4)$ and $[Cu^{II}L^{OMe3}](ClO_4)$. For all complexes,

Table 2 Comparison of selected bond lengths [Å] and angles [°] for $[Cu^{II}L^{napht2}](ClO_4)$, $[Cu^{II}L^{H3}](ClO_4)$, $[Cu^{II}L^{OMe3}](ClO_4)$, $[Cu^{II}L^{H4}](ClO_4)$ and $[Cu^{II}L^{H5}]_2(ClO_4)_2$ complexes

	$[Cu^{II}L^{napht2}](ClO_4)$	$[Cu^{II}L^{H3}](ClO_4)$	$[Cu^{II}L^{OMe3}](ClO_4)$	$[Cu^{II}L^{H4}](ClO)$	$[Cu^{II}L^{H5}]_2(ClO)_2$	Sq pyr Cu(II) in the literature	Ref.
Bond length [Å]							
M(1)–$N_{(imine)}$	1.9486(15)	1.989(3)	2.008(10)	1.929(2)	1.969(7)	1.923–1.969	14 and 31
M(1)–$N_{(py)}$	2.0122(16)	2.025(3)	2.014(11)	1.979(2)	2.006(7)	1.925–2.006	31 and 32
M(1)–$N_{(amine)}$	2.0910(15)	2.125(2)	2.148(9)	2.062(2)	2.057(7)	1.979–2.062	19 and 32–34
M(1)–$O_{(phenolic)}$	1.9234(12)	1.921(2)	1.927(8)	1.9172(17)	1.937(5)	1.917–2.096	19, 31 and 35–38
M(1)$\cdots O_{(hydroxyalkyl)}$	2.3802(13)	2.241(2)	2.222(9)	2.2195(18)	5.415	1.916–2.339	19
M(1)–$O_{(2)\#1}$					2.407(6)	2.423	38
M(1)$\cdots$M(1)					3.240	2.2729–3.001	19 and 31
Bond angle [°]							
$O_{(phenolic)}$–M(1)–$N_{(imine)}$	91.89(6)	90.19(9)	91.0(4)	95.54(8)	92.6(3)		
$O_{(phenolic)}$–M(1)–$N_{(py)}$	90.98(6)	88.29(10)	86.4(4)	94.89(8)	90.5(3)		
$N_{(imine)}$–M(1)–$N_{(py)}$	164.51(6)	159.96(11)	160.0(4)	155.64(9)	172.0(3)		
$O_{(phenolic)}$–M(1)–$N_{(amine)}$	170.51(6)	166.57(10)	164.0(4)	179.08(8)	165.4(3)		
$N_{(imine)}$–M(1)–$N_{(amine)}$	96.21(6)	102.86(11)	104.0(4)	86.37(9)	94.2(3)		
$N_{(py)}$–M(1)–$N_{(amine)}$	82.53(6)	80.54(11)	81.3(4)	84.27(8)	81.2(3)		
$O_{(phenolic)}$–M(1)–$O_{(hydroxyalkyl)}$	91.77(5)	94.75(9)	94.3(3)	90.62(7)			
$N_{(imine)}$–M(1)–$O_{(hydroxyalkyl)}$	109.15(5)	99.15(10)	97.1(4)	95.53(8)			
$N_{(py)}$–M(1)–$O_{(hydroxyalkyl)}$	85.96(5)	100.92(10)	102.9(4)	106.77(8)			
$N_{(amine)}$–M(1)–$O_{(hydroxyalkyl)}$	80.92(5)	80.2(9)	78.6(3)	89.27(7)			
$O_{(phenolic)}$–M(1)–$O_{(2)\#1}$					84.2(2)		
$N_{(imine)}$–M(1)–$O_{(2)\#1}$					91.0(2)		
$N_{(py)}$–M(1)–$O_{(2)\#1}$					96.7(2)		
$N_{(amine)}$–M(1)–$O_{(2)\#1}$					108.6(2)		

the N_{amine}–Cu–N_{py} angles are smaller than 90° [80.5–84.3°] for five membered chelate rings. The larger six-membered chelate rings lead to $O_{phenolic}$–Cu–N_{imine} angles that are all larger than 90° [90.2–94.5°]. A similar relationship between the N_{amine}–Cu–$O_{hydroxyalkyl}$ and also N_{amine}–Cu–N_{imine} angles and the different chelate ring sizes is described. In the case of $[Cu^{II}L^{napht2}](ClO_4)$, $[Cu^{II}L^{H3}](ClO_4)$ and $[Cu^{II}L^{OMe3}](ClO_4)$ complexes, involving the 2-hydroxyethyl arm, the N_{amine}–Cu–$O_{hydroxyalkyl}$ angles are smaller than 90° [78.6–80.9°] for five membered chelate rings, whilst in the $[Cu^{II}L^{H4}](ClO_4)$ complex involving the 3-hydroxypropyl arm, the N_{amine}–Cu–$O_{hydroxyalkyl}$ angle is ~90° [89.27°] for the six-membered ring. The N_{amine}–Cu–N_{imine} angle in $[Cu^{II}L^{H4}](ClO_4)$ involving the ethylamine chain [86.37°] is smaller than 90° for the five membered chelate ring, in $[Cu^{II}L^{napht2}](ClO_4)$ and $[Cu^{II}L^{H5}]_2(ClO_4)_2$ complexes, involving the propylamine chain [94.2–96.2°] and also in $[Cu^{II}L^{H3}](ClO_4)$ and $[Cu^{II}L^{OMe3}](ClO_4)$ complexes involving the butylamine chain [102.9–104.0°] is larger than 90° for six and seven membered chelate rings, respectively (Table 2). The square pyramid in Cu complexes is somewhat trigonally distorted, as shown by the degree of trigonality, (τ),[39–41] for Cu(1) being 0.10, 0.11, 0.066 and 0.39 for $[Cu^{II}L^{napht2}](ClO_4)$, $[Cu^{II}L^{H3}](ClO_4)$, $[Cu^{II}L^{OMe3}](ClO_4)$ and $[Cu^{II}L^{H4}](ClO_4)$, respectively.

Crystal structure of $[Cu^{II}L^{H5}]_2(ClO_4)_2$

Green single crystals of $[Cu^{II}L^{H5}]_2(ClO_4)_2$ were obtained by slow diffusion of diethyl ether into a solution of the complex dissolved in a mixture of CH_3CN and CH_3OH, and crystallise in the orthorhombic crystal system and the *Pbca* space group. The molecular structure and selected bond lengths and bond angles related to the coordination environment of the metal and also bond lengths related to similar compounds are given in Fig. 3 and Table 2, respectively. The structure is a dinuclear, comprising two similar Cu(II) centers. Each copper atom has a pentacoordinate square-pyramidal geometry. N(1), N(2), N(3) and O(2) of a deprotonated Schiff base bind four coordination sites of Cu(1). Similarly, Cu(2) is coordinated by N(1), N(2), N(3) and O(2) of another deprotonated Schiff base. The fifth, apical, coordination site of each Cu(1) is occupied by O(2) from another ligand, thereby forming a di-phenoxido-bridged dimer, while the hydroxypropyl arm (O(1)) of the ligand remains uncoordinated (Fig. 3). The charge distribution was assigned based on the presence of only two ClO_4^- anions which make the complex a dication with two deprotonated ligands L^{H5-}. Each phenoxy oxygen atom is bridging two complexes in an antisymmetric fashion giving Cu–$O_{phenoxy}$ bond lengths of 2.407 and 1.937 Å – which are in the range of previously reported structures for the copper(II) dimeric complex having a phenoxy bridge.[36–38] The coordination geometry around the copper centers is best described by the use of the τ-criterion,[37] indicating that the coordination geometry in $[Cu^{II}L^{H5}]_2^+$ is only slightly from square-pyramidal distorted (τ = 0.11). In this compound, N(1), N(2), N(3) and O(2) related to the same ligand occupy the equatorial positions and O(2)′, from the second ligand, occupies the apical position. The τ value for both Cu(1) in $[Cu^{II}L^{H5}]_2(ClO_4)_2$ is 0.11, which is similar to the value of Cu(II) in the monomers. Thus the geometries of both the copper centers in $[Cu^{II}L^{H5}]_2(ClO_4)_2$ are distorted square pyramidal. A 5,6,6-chelate ring sequence is observed in the dimer $[Cu^{II}L^{H5}]_2^+$, with the expected square-pyramidal coordination geometry for both Cu(II).

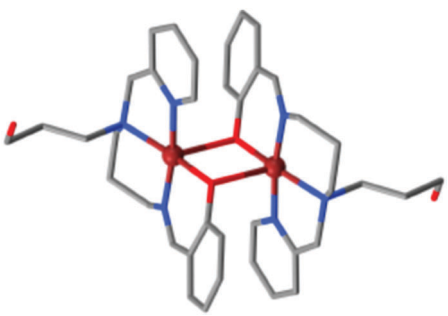

Fig. 3 Perspective of $[Cu^{II}L^{H5}]_2(ClO_4)_2$. Hydrogen atoms and anions are omitted for clarity. Cu, C, N and O are represented in dark red, gray, blue and red, respectively.

In contrast to coordinated ligands L^{napht2}, L^{H3}, L^{OMe3} and L^{H4} in $[Cu^{II}L^{napht2}](ClO_4)$, $[Cu^{II}L^{H3}](ClO_4)$, $[Cu^{II}L^{OMe3}](ClO_4)$ and $[Cu^{II}L^{H4}](ClO_4)$ complexes, respectively, the ligand anion in complex $[Cu^{II}L^{H5}]_2^+$ uses only four of the five donor groups binding to the copper atom, in which the hydroxypropyl arm remains uncoordinated and the phenolic oxygen atom bridges two Cu(II) atoms resulting in a Cu_2O_2 ring. This is not exclusively due to the steric situation in $[Cu^{II}L^{H5}]_2(ClO_4)_2$, but to the low stability of the six-membered chelate ring which would have been formed with the hydroxypropyl ligand arm: a similar behavior of related aliphatic tripodal ligands[10] and also asymmetric tripodal ligands with two aliphatic and one aromatic arms has been already reported.[26] In addition, the stability of the copper complex with the ligand **trpn**, which exclusively forms six-membered chelate rings, is shown to be about 10^5 times lower than the stability of the corresponding **tren** complex that contains only five-membered chelate rings.[9c] Examination of the Cu(II) complexes in the present study and the literature shows that Cu(II) atoms in tripodal complexes have a great flexibility in adoption of the number of chelate ring sequences around the metal atom to form a square pyramidal geometry around the central ion as observed for $[Cu^{II}L^{napht2}](ClO_4)$, 5,5,6,6, τ = 0.10; $[Cu^{II}L^{H3}]$ (ClO_4), 5,5,7,6, τ = 0.11; $[Cu^{II}L^{OMe3}](ClO_4)$, 5,5,7,6, τ = 0.066; $[Cu^{II}L^{H4}](ClO_4)$, 5,6,5,6, τ = 0.39 and $[Cu^{II}L^{H5}]_2(ClO_4)_2$, 5,6,6, τ = 0.11, but it should be noted that Cu(II) in these types of complexes is not stable against the high number of six-membered chelate rings around the metal.[9c] For the dinuclear complex $[Cu^{II}L^{H5}]_2(ClO_4)_2$ the hypothetical mononuclear $[Cu^{II}L^{H5}](ClO_4)$ would possess a 5,6,6,6 chelate ring sequence around the Cu(II) atom which, due to the high number of six-membered chelate rings, would be unstable. In order to form the stable structure with square pyramidal geometry, the hypothetical mononuclear complex would prefer to form a dinuclear structure with a 5,6,6 chelate ring sequence with a second identical ligand. Table 3 shows the comparison of the structural parameter (τ-value) for Cu(II) complexes characterized here.

Table 3 Comparison of the τ-value in 5-coordinated Cu complexes

5-Coordinated complexes	Chelate ring sequence	τ-Value
$[Cu^{II}L^{napht2}](ClO_4)$	5,5,6,6	0.10
$[Cu^{II}L^{H3}](ClO_4)$	5,5,7,6	0.11
$[Cu^{II}L^{OMe3}](ClO_4)$	5,5,7,6	0.066
$[Cu^{II}L^{H4}](ClO_4)$	5,6,5,6	0.39
$[Cu^{II}L^{H5}]_2(ClO_4)_2$	5,6,6	0.11

Theoretical studies

As described above, the present study brought us three interesting results. Firstly, we observed that the mononuclear five-coordinate complexes can be formed from most of ligands but dinuclear complexes only with a few of them. Secondly, X-ray crystal structures showed that hydrogen bonding can exist between two mononuclear five-coordinate complexes. Thirdly, mass spectra of both mononuclear and dinuclear complexes always show two characteristic peaks, one corresponding to a mononuclear fragment and one corresponding to a dinuclear fragment. In order to understand these results theoretical calculations were undertaken. The strength of interaction between two mononuclear four-coordinated fragments in one dinuclear complex and hydrogen bonding between two mononuclear five-coordinated complexes were evaluated (see Fig. 4). From this study it is clear that one of the coordinated arms in the mononulear complex leaves the metal ion and then the resulting four-coordinated complex can be dimerized. As can be seen in Fig. 3 and 4(a) in these dinuclear complexes, the hydroxyl group of the hydroxypropoyl arm is not coordinated to the metal ion. Thus the strength of the interaction between the hydroxyl group and the metal ion was evaluated, to figure out why it leaves the metal ion. However, the value of interaction energy between the metal ion and the whole ligand in these complexes was calculated first. As can be seen in Table 4, the values of interaction energies are relatively large and are in the range 629–634 kcal mol^{-1}. Thus in all mononuclear complexes the Schiff base ligands are tightly bonded to the central metal ion. However, the data show that the interaction energy between two mononuclear fragments in the dinuclear complex $[Cu^{II}L^{H5}]_2(ClO_4)_2$ is very small and only -4.24 kcal mol^{-1} (see Table 5). Such a small interaction energy is not surprising as the interacting fragments are both cations. This explains why even in the mass spectra of the dinuclear complexes the major peak corresponds to a mononuclear complex. Indeed, inside the mass spectrometer the dinuclear complex readily breaks into two mononuclear complexes. Two forms, **I** and **II**, were considered for one of the mononuclear fragments of the dinuclear complex $[Cu^{II}L^{H5}]_2(ClO_4)_2$ and the geometry was optimised for both of them (see Fig. 5e and f). The difference between the above forms is that in form **I** the hydroxyl group is not coordinated to the metal ion but is indeed coordinated in form **II**. The data showed that the energy difference between the above two forms is only -2.57 kcal mol^{-1}. Thus the interaction between the hydroxyl group and the central metal ion seems to be very weak. This means that the hydroxyl group simply leaves the metal ion, resulting in four-coordinated copper complexes which can be dimerized.

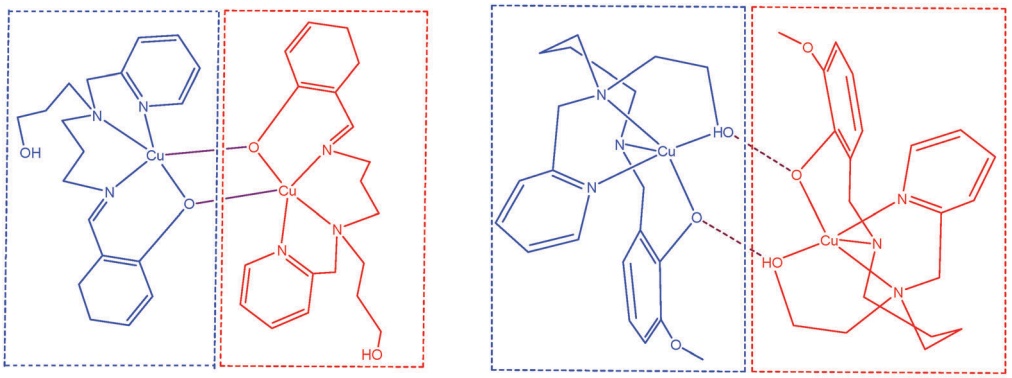

(a) IE = -4.24 kcal/mol (b) IE = -7.28 kcal/mol

Fig. 4 Interacting four-coordinated fragments in dinuclear complex $[Cu^{II}L^{H5}]_2(ClO_4)_2$ (a) and hydrogen bonding between two $[Cu^{II}L^{OMe3}](ClO_4)$ complexes (b).

Table 4 Calculated interaction energies (IE) between the metal ion and pentadentate ligands synthesized here

	E_{el} (Hartree)			
Compound	Cu^{2+}	L^{ald-} [a]	$[CuL^{ald}]^+$	IE (kcal mol^{-1})
$[Cu^{II}L^{OMe3}](ClO_4)$	−1639.151635	−1165.9898167	−2806.1509036	−633.44
$[Cu^{II}L^{H3}](ClO_4)$	−1639.151635	−1051.6149949	−2691.7726555	−631.29
$[Cu^{II}L^{napht2}](ClO_4)$	−1639.151635	−1165.7856412	−2805.939729	−629.05
$[Cu^{II}L^{H4}](ClO_4)$	−1639.151635	−1012.3607015	−2652.5239637	−634.81

[a] Frozen in the optimized geometry of the $[CuL^{ald}]^+$ complex.

Table 5 Calculated interaction energy (IE) between two $[Cu^{II}L^{OMe3}](ClO_4)$ complexes bonded through hydrogen bonding and also two mononuclear fragments in dinuclear $[Cu^{II}L^{H5}]_2(ClO_4)_2$

	E_{el} (Hartree)			
Compound	First complex/fragment[a]	Second complex/fragment[a]	Whole compound	IE (kcal mol^{-1})
$[Cu^{II}L^{OMe3}](ClO_4)$	−2806.1480886	−2806.1477506	−5612.3074422	−7.28
$[Cu^{II}L^{H5}]_2(ClO_4)_2$	−2691.7619224	−2691.7619224	−5383.5306096	−4.24

[a] Frozen in the optimized geometry of the whole compound.

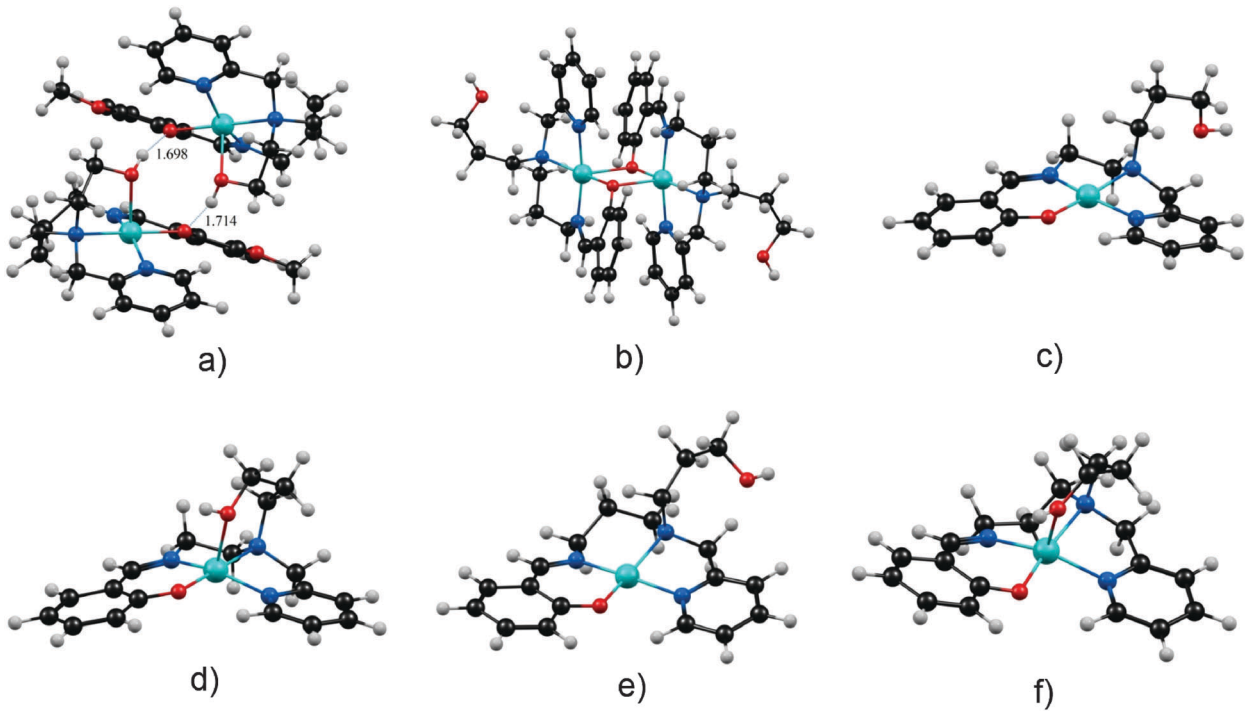

Fig. 5 The optimized structures of complexes/fragments studied here. (a) Two $[Cu^{II}L^{OMe3}](ClO_4)$ complexes bonded through hydrogen bonding. (b) Dinuclear $[Cu^{II}L^{H5}]_2(ClO_4)_2$ complex. (c) Form I of $[Cu^{II}L^{H4}](ClO_4)$. (d) Form II of $[Cu^{II}L^{H4}](ClO_4)$. (e) Form I of one fragment in $[Cu^{II}L^{H5}]_2(ClO_4)_2$. (f) Form II of one fragment in $[Cu^{II}L^{H5}]_2(ClO_4)_2$.

This is the reason why in mass spectra of all complexes there is a very small peak corresponding to a dinuclear complex.

Among the complexes synthesized here, both $[Cu^{II}L^{H5}]_2(ClO_4)_2$ and $[Cu^{II}L^{H4}](ClO_4)$ complexes have the hydroxyl group at the end of a propyl chain. For all the other complexes the hydroxyl group is at the end of an ethyl chain. Indeed, only in the case of $[Cu^{II}L^{H5}]_2(ClO_4)_2$ and $[Cu^{II}L^{H4}](ClO_4)$ we do observe an unstable six-membered chelate ring forming upon coordination of the hydroxyl group. For all other complexes the coordination of the hydroxyl group leads to the formation of a more stable five-membered chelate ring. Thus it seems that the formation of a dinuclear complex in which the hydroxyl group remained uncoordinated is quite expectable for both $[Cu^{II}L^{H5}]_2(ClO_4)_2$ and $[Cu^{II}L^{H4}](ClO_4)$ complexes. However X-ray crystal structure analysis confirmed the formation of a dinuclear complex only in the case of the former complex. Thus two forms **I** and **II** for $[Cu^{II}L^{H4}](ClO_4)$ were also considered and optimized (see Fig. 5c and d). As can be seen in Table 6, the data show that the energy difference between the above forms is about −5.32 kcal mol^{-1}.

Table 6 Calculated energy difference (ΔE) between the optimized structures of forms I and II considered here for mononuclear $[Cu^{II}L^{H4}](ClO_4)$ and one mononuclear fragment in dinuclear $[Cu^{II}L^{H5}]_2(ClO_4)_2$

	E_{el} (Hartree)		ΔE
Compound	Form I	Form II	(kcal mol^{-1})
$[Cu^{II}L^{H4}](ClO_4)$	−2691.7690481	−2691.7731458	−5.32
$[Cu^{II}L^{H5}]_2(ClO_4)_2$	−2652.5239637	−2652.5154793	−2.57

Thus it seems that the interaction energy between the hydroxyl group and the metal ion in complex $[Cu^{II}L^{H4}](ClO_4)$ is relatively large than that in complex $[Cu^{II}L^{H5}]_2(ClO_4)_2$. On the other hand, the interaction energy between two mononuclear fragments in the dinuclear complex $[Cu^{II}L^{H5}]_2(ClO_4)_2$ was only −4.24 kcal mol^{-1}. The above interaction is larger than −2.57 kcal mol^{-1} and less than −5.3 kcal mol^{-1}, calculated energy differences between forms **I** and **II** in complexes $[Cu^{II}L^{H5}]_2(ClO_4)_2$ and $[Cu^{II}L^{H4}](ClO_4)$, respectively. This explains why the complex $[Cu^{II}L^{H5}]_2(ClO_4)_2$ is dimerized while $[Cu^{II}L^{H4}](ClO_4)$ remained mononuclear. For

$[Cu^{II}L^{H5}]_2(ClO_4)_2$, in contrast to $[Cu^{II}L^{H4}](ClO_4)$, the value of interaction energy between two four coordinated fragments is larger than that between the hydroxyl group and the central metal ion.

In addition, we believe that the formation of hydrogen bonding between two mononuclear five-coordinated complexes prevents the formation of a dinuclear complex between two four-coordinated fragments. As seen in the previous section the X-ray crystal structure of the complex $[Cu^{II}L^{OMe3}](ClO_4)$ showed that the hydrogen bonding is formed between two mononuclear complexes. Indeed the coordination of the hydroxyl group to the metal ion and then the formation of the hydrogen bond between two molecules of such a five-coordinated complex in $[Cu^{II}L^{OMe3}](ClO_4)$ prevent the formation of a dinuclear complex which is formed in the case of $[Cu^{II}L^{H5}]_2(ClO_4)_2$. The value of the interaction between two mononuclear $[Cu^{II}L^{OMe3}](ClO_4)$ complexes due to hydrogen bonding is about -7.28 kcal mol^{-1} (see Fig. 4). Interestingly, the latter value is larger than -4.24 kcal mol^{-1}, and the interaction between two fragments in dinuclear complex $[Cu^{II}L^{H5}]_2(ClO_4)_2$ is larger than -2.57 and -5.3 kcal mol^{-1}, the energy difference between forms **I** and **II** of complexes $[Cu^{II}L^{H5}]_2(ClO_4)_2$ and $[Cu^{II}L^{H4}](ClO_4)$, respectively. Therefore these complexes are special cases in which the intermolecular interactions (herein hydrogen bonding) between two complexes can be stronger than some weak intramolecular metal–donor atom interactions. The formation of a mononuclear complex or a dinuclear one thus depends on the relative strength of inter- and intramolecular interactions.

Conclusion

In summary, we have reported the successful synthesis of 14 new mononuclear and a few dinuclear Cu(II) complexes by condensation of amines (**3–6**) with related aldehydes in the presence of Cu(II) metal ions. X-ray crystal structure determinations of $[Cu^{II}L^{napht2}](ClO_4)$, $[Cu^{II}L^{H3}](ClO_4)$, $[Cu^{II}L^{OMe3}](ClO_4)$ and $[Cu^{II}L^{H4}](ClO_4)$ revealed them to be monomeric, except for the dimeric $[Cu^{II}L^{H5}]_2(ClO_4)_2$. There is a distorted square pyramidal environment around the central ion in both mononuclear and dinuclear complexes. In this work, emphasis has been put on the examination of structural relationships in the complexation behavior. By comparing crystal structures of the complexes identified to date, it is found that all of them use four donor groups of the ligand (three nitrogen atoms and phenoxy oxygen atoms) to bind the metal atom and the differences observed are related to hydroxyalkyl arms. These arms are not coordinated to the metal ion in all complexes but in both the coordinated and non-coordinated state they remain protonated. Examination of X-ray crystal structures of Cu(II) complexes in the present study shows that in the Cu(II) complexes with an ethyl-amino arm, the hydroxypropyl group is bound to the Cu(II) atom, while in the Cu(II) complexes with a propyl-amino arm, the hydroxypropyl arm remains uncoordinated and a dinuclear Cu(II) complex is formed. According to the theoretical study, the interaction between the hydroxyl group and the central metal ion seems to be very weak thus the hydroxyl group can leave the metal ion, yielding four-coordinated Cu(II) complexes which can be dimerized. The theoretical study also showed that the formation of a mononuclear complex or a dinuclear one depends on the relative strength of inter- and intramolecular interactions. In Cu(II) complexes with a hydroxyethyl arm, there is a stronger interaction between the hydroxyl group and the central metal ion due to the formation of a stable five-membered chelate ring upon coordination of the hydroxyl group to the metal ion. In the case of the Cu(II) complexes with a hydroxypropyl arm, an unstable six-membered chelate ring forms upon coordination of the hydroxyl group – the formation of dinuclear structures is more expectable in this case. Note that both ligands L^{H5} and L^{H4} have a hydroxypropyl arm, but the X-ray crystal structure analysis confirmed the formation of a dinuclear copper complex only in the case of L^{H5}. By comparison of the structures, it seems that both aliphatic linkages are effective on the structure of dimeric complexes. According to theoretical studies, the value of interaction energy between two four coordinate fragments in the dinuclear $[Cu^{II}L^{H5}]_2(ClO_4)_2$ complex, in contrast to $[Cu^{II}L^{H4}](ClO_4)$, is larger than that between the hydroxyl group and the central metal ion. Thus we can assume that a mononuclear five coordinated complex forms first, and in a second time the hydroxyl group leaves the metal ion, resulting in a four-coordinated complex which can be dimerized. In addition to intramolecular interactions, intermolecular interactions are also important in the formation of a mononuclear complex or a dinuclear one. The theoretical study also supported our assumption that the formation of hydrogen bonds between two mononuclear five-coordinated complexes prevents the formation of a dinuclear complex between two four coordinate fragments.

Experimental

General remarks

Pyridine 2-carbaldehyde, 2-hydroxy-3-methoxybenzaldehyde, 2-hydroxybenzaldehyde, 2-hydroxy-1-naphthaldehyde and metal salt were obtained from Aldrich and used without further purification. 3,5-Di-*tert*-butyl-2-hydroxybenzaldehyde was synthesised according to the literature procedure.[42] All other chemicals and solvents were of reagent grade and were used as received except for methanol that was dried (Mg) before use.

Caution!

Whilst no problems were encountered in the course of this work, perchlorate mixtures are potentially explosive and should therefore be handled with appropriate care.

Infrared spectra were obtained between 4000 and 400 cm^{-1} on a Bruker Alpha FT-ATR IR spectrometer with a diamond anvil Alpha-P module for all complexese. UV-Vis spectra were recorded on a Jasco V550 spectrophotometer. ESI mass spectra were recorded at the University of Otago on a Bruker MicrOTOFQ spectrometer exception for $[Cu^{II}L^{H3}](ClO_4)$, $[Cu^{II}L^{OMe3}](ClO_4)$

and $[Cu^{II}L^{tBu3}](ClO_4)$ complexes that the spectra were recorded using a Kratos-MS-50T spectrometer. Room temperature magnetic moments were determined using a Johnson Matthey MSB-MK1 magnetic susceptibility balance. Standard microanalysis for all complexes was carried out using a Perkin-Elmer, CHNS/O elemental analyzer model 2400. ^1H and ^{13}C NMR spectra were taken in $CDCl_3$ on a Jeol 90 MHz spectrometer using $Si(CH_3)_4$ as an internal standard. Crystals suitable for X-ray diffraction were obtained by slow diffusion of diethyl ether vapor into methanol or a mixture of methanol and acetonitrile. Single crystal X-ray crystallographic data were collected at 100 K for $[Cu^{II}L^{napht2}](ClO_4)$, $[Cu^{II}L^{OMe3}](ClO_4)$ and $[Cu^{II}L^{H5}]_2(ClO_4)_2$ (λ = 1.54184) and also at 89 K for $[Cu^{II}L^{H4}](ClO_4)$ (λ = 0.71073) on a Bruker Kappa APEX II area detector diffractometer (University of Otago), using graphite monochromatic Mo-Kα radiation. In the case of the $[Cu^{II}L^{H3}](ClO_4)$ complex, single crystal X-ray crystallographic data were collected at 296 K (λ = 1.54184) on a Bruker SMART BREEZE CCD diffractometer using APEX2 software.[43] The data were collected for Lorentz and polarization effects and semi-empirical absorption corrections (SCALE) were applied. The structures were solved by direct or Patterson methods (SHELXS-97)[44] and refined against all F^2 data (SHELX-97).[45] All non-hydrogen atoms were modelled anisotropically except where noted. Unless otherwise specified, hydrogen atoms were inserted at calculated positions and rode on the atoms to which they were attached. In the case of this complex, absorption correction was applied to collected data using multi-scan, SADAPS V2012/1 software.[43] The title compound was solved by direct methods[46] using SHELXS-97 and refined using SHELXL-97.[46] The weighted *R*-factor, w*R* and goodness of fit *S* are based on F^2. The threshold expression of $F^2 > 2$ sigma (F^2) is used only for calculating *R*-factors. All estimated standard deviations (e.s.ds) are estimated using the full covariance matrix. The cell e.s.ds are taken into account individually in the estimation of e.s.d.s in distances, angles, and torsion angles; correlations between e.s.d.s in cell parameters are only used when they are defined by crystal symmetry. All non-hydrogen atoms were refined anisotropically and hydrogen atoms were added according to the theoretical model. In the case of complex $[Cu^{II}L^{OMe3}](ClO_4)$, we were not able to refine the X-ray crystal structure of this complex exactly.

Computational details

The crystallographic structure of all $[CuL^{aldi}]^+$ complexes was fully optimized using the def2-SVP basis set at the M06[47] level of theory. The calculated bond lengths and bond angles in optimized complexes were in good agreement with corresponding experimental data. Calculated root mean squares (RMSs) for metal–ligand bond distances were less than 0.055 (see Table 7). The interaction energy between the Cu^{2+} metal ion and the anionic ligand in mononulear complexes was calculated with the following equation:

$$\Delta E = E_{AB} - (E_A^{AB} + E_B^{AB}),$$

where E_{AB} is the minimized energy of the $[CuL^{aldi}]^+$ complexes and E_A^{AB} and E_B^{AB} are the energies of Cu^{2+} and L^- fragments, respectively, frozen in the geometry of this structure. Also interaction energies between the two mononuclear four coordinate fragments in one dinuclear $[Cu^{II}L^{H5}]_2(ClO_4)_2$ complex and two five coordinate $[Cu^{II}L^{OMe3}](ClO_4)$ complexes bonded through hydrogen bonding were calculated using the same formula, where E_{AB} is the minimized energy of the whole compound and E_A^{AB} and E_B^{AB} are the energies of the considered fragments. All calculations were performed using the Gaussian09 program.[48]

Table 7 Computed and experimental Cu–N and Cu–O bond lengths (Å) for $[CuL^{ald}]^+$ complexes[a]

Compounds	Cu–N_{amine}	Cu–N_{py}	Cu–N_{imine}	Cu–O^-	Cu–OH	RMS
$[Cu^{II}L^{OMe3}](ClO_4)$	2.190	2.045	2.009	1.944	2.209	0.041
	2.136	*2.039*	*2.013*	*2.013*	*2.232*	
$[Cu^{II}L^{H3}](ClO_4)$	2.227	2.046	1.985	1.916	2.298	0.054
	2.125	*2.025*	*1.990*	*1.921*	*2.236*	
$[Cu^{II}L^{napht2}](ClO_4)$	2.140	2.030	1.940	1.916	2.339	0.030
	2.091	*2.012*	*1.949*	*1.923*	*2.380*	
$[Cu^{II}L^{H4}](ClO_4)$	2.113	2.017	1.935	1.905	2.250	0.032
	2.062	*1.979*	*1.928*	*1.917*	*2.220*	
$[Cu^{II}L^{H5}]_2(ClO_4)_2$	2.102	2.027	1.988	1.975	2.340[b]	0.042
	2.056	*2.006*	*1.970*	*1.938*	*2.407*	

[a] The data obtained at the M06/def2-SVP level are given as a plain text and experimental data are in italic. [b] For this complex this is the distance between Cu(1)–O-(2) bonds.

Synthesis and characterization

General synthesis of unsymmetrical tripodal amines (3–6). 2-Aminoethanol (1.22 g, 20 mmol) or 3-aminopropan-1-ol (1.50 g, 20 mmol) in dry EtOH (100 mL) was added dropwise to a solution of pyridine-2-carbaldehyde (2.14 g, 20 mmol) in dry EtOH (100 mL) over a period of 2 h separately. The mixture was refluxed under stirring for 12 h. Solid sodium borohydride (3.02 g, 80 mmol) was then added slowly and the reaction mixture was stirred for a further 12 h before it was filtered. The filtrate was reduced to 20 mL by rotary evaporation. Water (50 mL) was added and the products were extracted with chloroform (3 × 50 mL). The combined extracts were dried over magnesium sulfate, filtered, and then dried by rotary evaporation. The resulting brown oil (1.52 g, 10 mmol (starting with 2-aminoethano, **l′**) or 1.66 g, 10 mmol (starting with 3-aminopropan-1-ol, **2′**), 77–86%) was dissolved in acetonitrile (70 mL), solid K_2CO_3 (2.07 g, 15 mmol) was added, and the mixture brought to reflux before a solution of *N*-(4-bromobutyl)-phthalimide (2.81 g, 10 mmol) was added dropwise to **l′**, or *N*-(2-bromoethyl)phthalimide (2.53 g, 10 mmol) or *N*-(3-bromopropyl)phthalimide (2.67 g, 10 mmol) or *N*-(4-bromobutyl)-phthalimide (2.81 g, 10 mmol) in acetonitrile (70 mL) to **2′**. The mixture was refluxed for 48 h and then filtered hot. The filtrate was reduced to dryness by rotary evaporation. The brown oil residue was boiled under reflux for 12 h in aqueous HCl (25%, 100 mL) then evaporated to a small volume (*ca.* 25 mL) under vacuum and cooled in a refrigerator for several hours. The resulting solid was filtered off and discarded, and the filtrate was evaporated to dryness under vacuum. Water (50 mL) was added to the resulting brown residue and the pH was adjusted to 12 with sodium hydroxide before extracting with chloroform (3 × 50 mL). The combined extract was dried over magnesium sulfate, and

filtered and the chloroform was removed from the filtrate by rotary evaporation to leave the products, **3–6**, as brown oils.

Synthesis of 2-((4-aminobutyl)(pyridin-2-ylmethyl)amino)-ethanol (3). Yield: 1.34 g (60%). Anal. calc. for $C_{12}H_{21}N_3O$ (M_w: 223.17): C, 64.54; H, 9.48; N, 18.82. Found: 64.35; H, 9.25; N, 19.10%. IR (Nujol mull, cm^{-1}) 3354, 3272 $\nu(NH_2)$, 1591 $\nu(C{=}N)_{py}$. ^1H NMR ($CDCl_3$, ppm) δ = 1.36–1.55 (m, 4H); 2.33 (b, 3H), 2.55–2.72 (m, 6H); 3.58–3.60 (t, 2H); 3.78 (s, 2H); 7.14–7.17 (m, 1H); 7.14–7.17 (t, 1H); 7.29 (d, 1H); 7.62–7.66 (td, 1H); 8.52 (d, 1H). ^{13}C NMR ($CDCl_3$, ppm) δ = 24.057; 29.248; 40.432; 54.065; 56.110; 58.750; 59.688; 121.349, 122.493; 135.879; 148.314; 159.228.

Synthesis of 3-((2-aminoethyl)(pyridin-2-ylmethyl)amino)propan-1-ol (4). Yield: 1.61 g (77%). Anal. calc. for $C_{11}H_{19}N_3O$ (M_w: 209.15): C, 63.13; H, 9.15; N, 20.08. Found: 64.05; H, 9.25; N, 19.70%. IR (Nujol mull, cm^{-1}) 3341, 3262 $\nu(NH_2)$, 1593 $\nu(C{=}N)_{py}$. ^1H NMR ($CDCl_3$, ppm) δ = 1.309–1.625 (m, 2H); 2.432–2.631 (m, 6H); 3.334–3.640 (m, 4H); 4.466 (s, 3H); 6.837–7.403 (m, 3H); 8.234 (d, 1H). ^{13}C NMR ($CDCl_3$, ppm) δ = 29.061; 38.186; 51.476; 54.671; 59.340; 59.826; 121.420, 122.367; 135.981; 148.220; 158.791.

Synthesis of 3-((3-aminopropyl)(pyridin-2-ylmethyl)amino)-propan-1-ol (5). Yield: 1.92 g (86%). Anal. calc. for $C_{12}H_{21}N_3O$ (M_w: 223.31): C, 64.54; H, 9.48; N, 18.82. Found: 64.20; H, 9.65; N, 18.90%. IR (Nujol mull, cm^{-1}) 3352, 3271 $\nu(NH_2)$, 1591 $\nu(C{=}N)_{py}$. ^1H NMR ($CDCl_3$, ppm) δ = 1.497 (m, 4H); 2.309–2.546 (m, 6H); 3.482 (s, 4H); 4.436 (s, 3H); 6.856–7.505 (m, 3H); 8.299 (d, 1H). ^{13}C NMR ($CDCl_3$, ppm) δ = 25.886; 28.631; 39.169; 50.729; 51.830; 59.026; 59.715; 121.485, 122.507; 136.132; 148.245; 158.371.

Synthesis of 3-((4-aminobutyl)(pyridin-2-ylmethyl)amino)-propan-1-ol (6). Yield: 1.73 g (73%). Anal. calc. for $C_{13}H_{23}N_3O$ (M_w: 237.18): C, 65.79; H, 9.77; N, 17.70. Found: 65.10; H, 9.45; N, 17.20%. IR (Nujol mull, cm^{-1}) 3360, 3288 $\nu(NH_2)$ 1591 $\nu(C{=}N)_{py}$. ^1H NMR ($CDCl_3$, ppm) δ = 1.324–1.503 (m, 6H); 2.275–2.454 (m, 6H); 3.505 (s, 4H); 4.538 (s, 3H); 6.960–7.455 (m, 3H); 8.298 (s, 1H). ^{13}C NMR ($CDCl_3$, ppm) δ = 23.495; 28.598; 29.624; 40.283; 51.612; 53.237; 59.436; 60.711, 121.218; 122.362; 135.758; 148.031, 158.747.

General synthesis of the complexes

A solution of 0.5 mmol of appropriate aldehyde, 2-hydroxy-3-methoxy-benzaldehyde (0.08 g, 0.5 mmol), 2-hydroxybenzaldehyde (0.06 g, 0.5 mmol), 3,5-di-*tert*-butyl-2-hydroxybenzaldehyde (0.117 g, 0.5 mmol) or 2-hydroxy-1-naphthaldehyde (0.086 g, 0.5 mmol) in methanol (50 ml) and 7 drops of $N(Et)_3$ were added dropwise to a refluxing solution of $Cu(ClO_4)_2{\cdot}6H_2O$ (0.184 g, 0.5 mmol) and the corresponding amine, **1** (0.098 g, 0.5 mmol) or **2** (0.105 g, 0.5 mmol) or **3** (0.112 g, 0.5 mmol) or **4** (0.105 g, 0.5 mmol) or **5** (0.112 g, 0.5 mmol) or **6** (0.119 g, 0.5 mmol) in the same solvent (50 mL). After refluxing for 12 h, the solution was concentrated in a rotary evaporator (**EXTREME CAUTION!**) at room temperature to *ca.* 5–10 mL. A small volume of diethyl ether was added slowly, producing a powdery precipitate. The powdery Cu(II) products were filtered off, washed with cold diethyl ether and dried under vacuum. Crystalline or powdery compounds were obtained by slow diffusion of diethyl ether vapor into a solution of these compounds in methanol or a mixture of methanol and acetonitrile, as detailed below.

$[Cu^{II}L^{naph1}](ClO_4)$. Recrystallisation of the initial solid from a mixture of CH_3OH and MeCN in a 5 : 1 ratio *via* slow vapour diffusion of Et_2O yields green powder (0.10 g, 79.8%). Anal. calc. for $C_{21}H_{22}ClCuN_3O_6$: C, 49.32; H, 4.34; N, 8.22. Found: C, 49.77; H, 4.55; N, 7.92%. IR (ATR, cm^{-1}) 1616 $\nu(C{=}N)_{imi}$, 1604, 1458 $\nu(C{=}N)_{py}$ and $\nu(C{=}C)$, 1088, 620 $\nu(ClO_4^-)$. ESI-MS (MeOH, m/z^+): 411.1 $[Cu^{II}L^{naph1}]^+$. UV-Vis {λ_{max}, nm (ε_{max}, M^{-1} cm^{-1})} in CH_3CN: 228 (21 097), 390 (2572), 572 (116). Magnetic moment: μ_{eff} = 2.2 BM [Gouy].

$[Cu^{II}L^{naph2}](ClO_4)$. Recrystallisation of the initial solid from CH_3OH *via* slow vapour diffusion of Et_2O yields green crystals (0.11g, 83.7%). Anal. calc. for $C_{22}H_{24}ClCuN_3O_6$: C, 50.29; H, 4.60; N, 8.00. Found: C, 50.22; H, 4.49; N, 7.97%. IR (ATR, cm^{-1}) 1616 $\nu(C{=}N)_{imi}$; 1449 $\nu(C{=}N)$ and $\nu(C{=}C)$, 1088, 619 $\nu(ClO_4)$. ESI-MS (MeOH, m/z^+): 425.1 $[Cu^{II}L^{naph2}]^+$, 851.2 $([Cu^{II}L^{naph2}]^+_2 + H)$, 949.2 $([Cu^{II}L^{naph2}]^+_2)ClO_4$. UV-Vis {$\lambda_{max}$, nm ($\varepsilon_{max}$, M^{-1} cm^{-1})} in CH_3CN: 298 (17 419), 387 (6369), 583 (141). Magnetic moment: μ_{eff} = 1.72 BM [Gouy].

$[Cu^{II}L^{H3}](ClO_4)$. Recrystallisation of the initial solid from CH_3OH *via* slow vapour diffusion of Et_2O yields green crystals (0.08 g, 62%). Anal. calc. for $C_{19}H_{24}ClCuN_3O_6$: C, 46.63; H, 4.94; N, 8.59. Found: C, 46.62; H, 5.12; N, 8.39%. IR (ATR, cm^{-1})1619 $\nu(C{=}N)_{imi}$; 1450 $\nu(C{=}C)_{py}$, 1080, 620$\nu(ClO_4)$. ESI-MS (MeOH, m/z^+): 389.1 $[CuL^{H3}]^+$, 777.2 $([CuL^{H3}]_2{}^-H)^+$, 879.2 $([Cu^{II}L^{H3}]_2 + 2H)ClO_4^+$. UV-Vis {$\lambda_{max}$, nm ($\varepsilon_{max}$, M^{-1} cm^{-1})} in CH_3CN: 224 (137 236), 272 (25 701), 374 (1377), 463 (314.12), 612 (128.46), 761 (76.53). Magnetic moment: μ_{eff} = 1.84 BM [Gouy].

$[Cu^{II}L^{OMe3}](ClO_4)$. Recrystallisation of the initial solid from a mixture of CH_3OH and MeCN in a 1 : 1 ratio *via* slow vapour diffusion of Et_2O yields green crystals (0.10 g, 80%). Anal. calc. for $C_{20}H_{26}ClCuN_3O_7$: C, 46.25; H, 5.05; N, 8.09. Found: C, 45.39; H, 5.29; N, 7.72%. IR (ATR, cm^{-1}): 1615 $\nu(C{=}N)_{imi}$; 1600, 1454 $\nu(C{=}N)_{py}$ and $\nu(C{=}C)$, 1078, 621 $\nu(ClO_4)$. ESI-MS (MeOH, m/z^+): 419.1 $[Cu^{II}L^{OMe3}]^+$, 837.3 $([Cu^{II}L^{OMe3}]_2 - H)^+$, 939.2 $([Cu^{II}L^{OMe3}]_2 + 2H)ClO_4^+$. UV-Vis {$\lambda_{max}$, nm ($\varepsilon_{max}$, M^{-1} cm^{-1})} in CH_3CN: 238 (31 324), 281 (18 414), 384 (2537), 483 (303.65), 602 (133.7), 781 (94). Magnetic moment: μ_{eff} = 2 BM [Gouy].

$[Cu^{II}L^{tBu3}](ClO_4)$. Recrystallisation of the initial solid from CH_3OH *via* slow vapour diffusion of Et_2O yields green powder (0.11 g, 73%). Anal. calc. for $C_{27}H_{40}ClCuN_3O_6$: C, 53.90; H, 6.70; N, 6.98. Found: C, 53.46; H, 6.63; N, 7.32%. IR (ATR, cm^{-1}): 1617 $\nu(C{=}N)_{imi}$; 1441 $\nu(C{=}C)$, 1085, 622 $\nu(ClO_4)$. ESI-MS (MeOH, m/z^+): 501.2 $[Cu^{II}L^{tBu3}]^+$, 1001.5 $([Cu^{II}L^{tBu3}]_2 - H)^+$, 1103.4 $([Cu^{II}L^{tBu3}]_2 + 2H)ClO_4^+$. UV-Vis {$\lambda_{max}$, nm ($\lambda_{max}$, M^{-1} cm^{-1})} in CH_3CN: 228 (15 389), 247 (14 363.4), 279 (9711.6), 320 (3988), 381 (3323), 486 (122), 633 (121), 819 (60). Magnetic moment: μ_{eff} = 1.88 BM [Gouy].

$[Cu^{II}L^{naph3}](ClO_4){\cdot}0.25CH_3OH$. Recrystallisation of the initial solid from a mixture of CH_3OH and CH_3CN in a 2 : 1 ratio *via* slow vapour diffusion of Et_2O yields green powder (0.09 g, 68%). Anal. calc. for $C_{23.25}H_{27}ClCuN_3O_{6.25}$: C, 51.01; H, 4.97; N, 7.68. Found: C, 51.2; H, 4.92; N, 7.73%. IR (ATR, cm^{-1}, cm^{-1}) 1615 $\nu(C{=}N)_{imi}$; 1604, 1447 $\nu(C{=}N)_{py}$ and $\nu(C{=}C)$, 1079, 620 $\nu(ClO_4)$. ESI-MS (MeOH, m/z^+): 439.1 $[Cu^{II}L^{naph3}]^+$,

879.3 ($[Cu^{II}L^{napht3}]_2$ + H)$^+$, 979.2 ($[Cu^{II}L^{napht3}]_2$ + 2H)ClO_4^+. UV-Vis {λ_{max}, nm (ε_{max}, M^{-1} cm^{-1})} in CH_3CN: 238 (35 335), 311 (17 908), 398 (6036), 485 (sh), 600 (157), 770 (98). Magnetic moment: μ_{eff} = 2.01 BM [Gouy].

$[Cu^{II}L^{H4}](ClO_4)$. Recrystallisation of the initial solid from a mixture of CH_3OH and CH_3CN in a 1 : 1 ratio *via* vapour diffusion of Et_2O yields green crystals (0.178 g, 75%). Anal. calc. for $C_{18}H_{22}ClCuN_3O_6$: C, 45.48; H, 4.66; N, 8.84. Found: C, 45.42; H, 4.93; N, 9.02%. IR (ATR, cm^{-1}): 1632 ν(C═N)$_{imi}$, 1600, 1445 ν(C═N)$_{py}$ and ν(C═C), 1071, 619 $\nu(ClO_4)$. ESI-MS (MeOH, m/z^+): 375.1 $[Cu^{II}L^{H4}]^+$. UV-Vis {λ_{max}, nm (ε_{max}, M^{-1} cm^{-1})} in CH_3CN: 222 (18 271), 244 (17 469), 266 (14 079), 371 (3402), 587 (169). Magnetic moment: μ_{eff} = 1.82 BM [Gouy].

$[Cu^{II}L^{OMe4}](ClO_4)$. Recrystallisation of this solid from CH_3OH *via* slow vapour diffusion of Et_2O yields green crystals (0.095 g, 75%). Anal. calc. for $C_{19}H_{24}ClCuN_3O_7$: C, 45.15; H, 4.79; N, 8.31. Found: C, 45.29; H, 4.60; N, 8.40%. IR (ATR, cm^{-1}); 1622 ν(C═N)$_{imi}$; 1444 ν(C═N)$_{py}$ and ν(C═C), 1068, 620 $\nu(ClO_4)$. ESI-MS (MeOH, m/z^+): 405.1 $[Cu^{II}L^{OMe4}]^+$. UV-Vis {λ_{max}, nm (ε_{max}, M^{-1} cm^{-1})} in CH_3CN: 205 (22 476), 240 (17 281), 270 (12 011), 382 (2324), 575 (174). Magnetic moment: μ_{eff} = 1.90 BM [Gouy].

$[Cu^{II}L^{tBu3}](ClO_4)\cdot 0.1CH_3OH$. Recrystallisation of the initial solid from CH_3OH *via* slow vapour diffusion of Et_2O yields green powder (0.115 g, 78%). Anal. calc. for $C_{26.1}H_{38.4}ClCuN_3O_{6.1}$: C, 53.06; H, 6.55; N, 7.11. Found: C, 53.16; H, 6.63; N, 7.02%. IR (ATR, cm^{-1}): 1629 ν(C═N)$_{imi}$; 1612, 1462 ν(C═N)$_{py}$ and ν(C═C), 1070, 620 $\nu(ClO_4)$. ESI-MS (MeOH, m/z^+): 487.2 $[Cu^{II}L^{Bu4}]^+$. UV-Vis {λ_{max}, nm (ε_{max}, M^{-1} cm^{-1})} in CH_3CN: 227 (17 049), 248 (14 636), 274 (10 800), 383 (3105), 630 (155). Magnetic moment: μ_{eff} = 1.95 BM [Gouy].

$[Cu^{II}L^{napht4}](ClO_4)$. Recrystallisation of the initial solid from a mixture of CH_3OH and CH_3CN in a 3 : 1 ratio *via* slow vapour diffusion of Et_2O yields green powder (0.191 g, 73%). Anal. calc. for $C_{22}H_{24}ClCuN_3O_6$: C, 50.29; H, 4.60; N, 8.00. Found: C, 50.67; H, 4.72; N, 7.73%. IR (ATR, cm^{-1}): 1618 ν(C═N)$_{imi}$; 1607, 1437 ν(C═N)$_{py}$ and ν(C═C), 1072, 619 $\nu(ClO_4^-)$. ESI-MS (MeOH, m/z^+): 425.1 $[Cu^{II}L^{napht4}]^+$, 951.2 $([Cu^{II}L^{napht4}]_2ClO_4 + 2H)^+$. UV-Vis {$\lambda_{max}$, nm ($\varepsilon_{max}$, M^{-1} cm^{-1})} in CH_3CN: 226 (27 244), 237 (sh), 248 (sh), 287 (10 913), 313 (8927), 383 (4194), 574 (162). Magnetic moment: μ_{eff} = 1.86 BM [Gouy].

$[Cu^{II}L^{H5}]_2(ClO_4)_2$. Recrystallisation of the initial solid from a mixture of CH_3CN and CH_3OH in a 5 : 1 ratio *via* vapour diffusion of Et_2O yields green crystals (0.342 g, 70%). Anal. calc. for $C_{38}H_{48}Cl_2Cu_2N_6O_{12}$: C, 46.63; H, 4.94; N, 8.59. Found: C, 46.72; H, 4.90; N, 9.01%. IR (KBr disc, cm^{-1}): 1620 ν(C═N)$_{imi}$; 1596, 1440 ν(C═N)$_{py}$ and ν(C═C), 1069, 619 $\nu(ClO_4)$. ESI-MS (MeOH, m/z^+): 389.1 $[Cu^{II}L^{H5}]^+$, 879.1 $([Cu^{II}L^{H5}]_2ClO_4 + 2H)^+$. UV-Vis {$\lambda_{max}$, nm ($\varepsilon_{max}$, M^{-1} cm^{-1})} in CH_3CN: 257 (6806), 305 (2924), 404 (379), 598 (92). Magnetic moment: μ_{eff} = 1.58 B.M per Cu atom [Gouy].

$[Cu^{II}L^{OMe5}]_2(ClO_4)_2$. Recrystallisation of the initial solid from a mixture of CH_3OH and MeCN in a 5 : 1 ratio *via* slow vapour diffusion of Et_2O yields green powder (0.348 g, 67%). Anal. calc. for $C_{40}H_{52}Cl_2Cu_2N_6O_{14}$: C, 46.25; H, 5.05; N, 8.09. Found: C, 46.17; H, 5.25; N, 8.4%. IR (ATR, cm^{-1}): 1620 ν(C═N)$_{imi}$; 1444 ν(C═C), 1078, 620 $\nu(ClO_4)$. ESI-MS (MeOH, m/z^+): 419.1 $[Cu^{II}L^{OMe5}]^+$, 939.2 $([Cu^{II}L^{OMe5}]_2 + 2H)ClO_4^+$. UV-Vis {$\lambda_{max}$, nm ($\varepsilon_{max}$, M^{-1} cm^{-1})} in CH_3CN: 258 (9704), 313 (3700), 406 (754), 587 (122). Magnetic moment: μ_{eff} = 1.52 BM per Cu atom [Gouy].

$[Cu^{II}L^{tBu5}]_2(ClO_4)_2$. Recrystallisation of the initial solid from CH_3OH *via* slow vapour diffusion of Et_2O yields green crystals (0.189 g, 63%). Anal. calc. for $C_{54}H_{80}Cl_2Cu_2N_6O_{12}$: C, 53.90; H, 6.70; N, 6.98. Found: C, 53.65; H, 6.93; N, 7.22%. IR (ATR, cm^{-1}): 1624 ν(C═N)$_{imi}$; 1600, 1440 ν(C═N)$_{py}$ and ν(C═C), 1074, 620 $\nu(ClO_4)$. ESI-MS (MeOH, m/z^+): 501.2 $[Cu^{II}L^{tBu5}]^+$. UV-Vis {λ_{max}, nm (ε_{max}, M^{-1} cm^{-1})} in CH_3CN: 210 (127 302), 229 (14 206), 248 (13 790), 275 (9945), 306 (4208), 383 (2838), 610 (166). Magnetic moment: μ_{eff} = 1.32 BM per Cu atom [Gouy].

$[Cu^{II}L^{napht5}]_2(ClO_4)_2$. Recrystallisation of the initial solid from CH_3OH *via* slow vapour diffusion of Et_2O yields green powder (0.177 g, 66%). Anal. calc. for $C_{46}H_{52}Cl_2Cu_2N_6O_{12}$: C, 51.21; H, 4.86; N, 7.79. Found: C, 51.62; H, 4.93; N, 8.03%. IR (ATR, cm^{-1}): 1620 ν(C═N)$_{imi}$; 1602, 1449 ν(C═N)$_{py}$ and ν(C═C), 1079, 620 $\nu(ClO_4^-)$. ESI-MS (MeOH, m/z^+): 439.1 $[Cu^{II}L^{napht5}]^+$, 979.2 $([Cu^{II}L^{napht5}]_2 + 2H)ClO_4^+$. UV-Vis {$\lambda_{max}$, nm ($\varepsilon_{max}$, M^{-1} cm^{-1})} in CH_3CN: 224 (36 505), 322 (10 751), 382 (4649), 402 (sh), 599 (140). Magnetic moment: μ_{eff} = 1.66 BM Cu atom [Gouy].

$[Cu^{II}L^{H6}](ClO_4)$. Recrystallisation of the initial solid from CH_3OH *via* slow vapour diffusion of Et_2O yields green powder (0.16 g, 65%). Anal. calc. for $C_{20}H_{26}ClCuN_3O_6$: C, 47.71; H, 5.21; N, 8.35. Found: C, 47.62; H, 5.42; N, 8.19%. IR (ATR, cm^{-1}) 1624 ν(C═N)$_{imi}$; 1446 ν(C═C), 1049, 620 $\nu(ClO_4)$. ESI-MS (MeOH, m/z^+): 403.1326 $[CuL^{H6}]^+$. UV-Vis {λ_{max}, nm (ε_{max}, M^{-1} cm^{-1})} in CH_3CN: 223 (49 480), 273 (15 334), 307 (5202), 371 (3433), 619 (136). Magnetic moment: μ_{eff} = 1.78 BM [Gouy].

$[Cu^{II}L^{OMe6}](ClO_4)\cdot 0.25CH_3OH$. Recrystallisation of the initial solid from a mixture of CH_3OH and MeCN in a 1 : 1 ratio *via* slow vapour diffusion of Et_2O yields green powder (0.18 g, 68%). Anal. calc. for $C_{21.25}H_{29}ClCuN_3O_{7.25}$: C, 47.14; H, 5.40; N, 7.76. Found: C, 47.24; H, 5.39; N, 7.72%. IR (ATR, cm^{-1}): 1615 ν(C═N)$_{imi}$; 1446 ν(C═C), 1074, 625 $\nu(ClO_4)$. ESI-MS (MeOH, m/z^+): 433.1411 $[Cu^{II}L^{OMe6}]^+$. UV-Vis {λ_{max}, nm (ε_{max}, M^{-1} cm^{-1})} in CH_3CN: 204 (23 919), 237 (21 533), 281 (13 442), 381 (3564), 594 (145). Magnetic moment: μ_{eff} = 1.74 BM [Gouy].

$[Cu^{II}L^{tBu6}](ClO_4)\cdot 0.25H_2O$. Recrystallisation of the initial solid from CH_3OH *via* slow vapour diffusion of Et_2O yields green powder (0.19 g, 63%). Anal. calc. for $C_{28}H_{42.5}ClCuN_3O_{6.25}$: C, 54.23; H, 6.91; N, 6.78. Found: C, 54.23; H, 6.91; N, 6.78%. IR (ATR, cm^{-1}): 1613 ν(C═N)$_{imi}$; 1460 ν(C═C), 1081, 621 $\nu(ClO_4)$. ESI-MS (MeOH, m/z^+): 515.2532 $[Cu^{II}L^{tBu6}]^+$. UV-Vis {λ_{max}, nm (ε_{max}, M^{-1} cm^{-1})} in CH_3CN: 203 (19 536), 228 (15 706), 248 (14 105), 280 (9412), 328 (3974), 384 (3135), 507 (165), 621 (164). Magnetic moment: μ_{eff} = 1.92 BM [Gouy].

$[Cu^{II}L^{napht6}](ClO_4)$. Recrystallisation of the initial solid from a mixture of CH_3OH and CH_3CN in a 3 : 1 ratio *via* slow vapour diffusion of Et_2O yields green powder (0.19 g, 69%). Anal. calc. for $C_{24}H_{28}ClCuN_3O_6$: C, 52.08; H, 5.10; N, 7.59. Found: C, 52.42; H, 5.22; N, 7.33%. IR (ATR, cm^{-1}, cm^{-1}) 1622 ν(C═N)$_{imi}$; 1597, 1445 ν(C═N)$_{py}$ and ν(C═C), 1051, 619 $\nu(ClO_4)$. ESI-MS (MeOH, m/z^+): 453.1437 $[Cu^{II}L^{napht6}]^+$. UV-Vis {λ_{max}, nm (ε_{max}, M^{-1} cm^{-1})}

in CH_3CN: 227 (26 485), 235 (26 573), 311 (12 151), 383 (4209), 399 (4221), 588 (112). Magnetic moment: μ_{eff} = 2.02 BM [Gouy].

Acknowledgements

We are grateful to the Faculty of Chemistry of Bu-Ali Sina University, Ministry of Science, Research and Technology of Iran, the University of Otago and the MacDiarmid Institute for Advanced Materials and Nanotechnology for financial support (PhD scholarship for SD), and Professor Sally Brooker for hosting MS for a 6-month research visit.

Notes and references

1 (*a*) L. F. Szczepura, L. M. Witham and K. J. Takeuchi, *Coord. Chem. Rev.*, 1998, **174**, 5–32; (*b*) J. M. Baumeister, R. Alberto, K. Ortner, B. Spingler, P. A. Schubiger and T. A. Kaden, *J. Chem. Soc., Dalton Trans.*, 2002, 4143–4151; (*c*) I. Yoon, Y. W. Shin, J. Kim, K.-M. Park, S. B. Park and S. S. Lee, *Acta Crystallogr., Sect. C: Cryst. Struct. Commun.*, 2002, **58**, m165–m166; (*d*) K. S. Choi, D. Kang, J.-E. Lee, J. Seo and S. S. Lee, *Bull. Korean Chem. Soc.*, 2006, **27**, 747–754; (*e*) S. Chung, W. Kim, S. B. Park, I. Yoon, S. S. Lee and D. D. Sung, *J. Chem. Soc., Chem. Commun.*, 1997, 965–966; (*f*) S. S. Lee, J. M. Park, D. Y. Kim, J. H. Jung and M. H. Cho, *Chem. Lett.*, 1995, 1009–1010; (*g*) Y.-S. Xie, H. Jiang, X.-T. Liu, Z.-Y. Zhou, Q.-L. Liu and X.-L. Xu, *Collect. Czech. Chem. Commun.*, 2002, **67**, 1647–1657.

2 S. Paul, A. K. Barik, R. J. Butcher and S. K. Kar, *Polyhedron*, 2000, **19**, 2661–2666.

3 L. R. Gahan, T. M. Donlevy and T. W. Hambley, *Inorg. Chem.*, 1990, **19**, 1451–1454.

4 A. M. Sargeson, *Pure Appl. Chem.*, 1984, **56**, 1603–1619.

5 K. Ziegler, *Methodes der Organischen Chemie, Part 2*, Houben-weyl, Georg-Thieme-Verlag, Stuttgart, 1955, vol. 4, p.729.

6 J. Hunter, J. Nelson, C. Harding, M. McCann and V. McKee, *J. Chem. Soc., Chem. Commun.*, 1990, 1148–1151.

7 T. M. Garrett, T. J. McMurry, M. W. Hosseini, Z. E. Reyes, F. E. Hahn and K. N. Raymond, *J. Am. Chem. Soc.*, 1991, **113**, 2965–2977.

8 L. Busetto and V. Zanotti, *Inorg. Chim. Acta*, 2008, **361**, 3004–3011.

9 (*a*) R. L. Fanshawe and A. G. Blackman, *Inorg. Chem.*, 1995, **34**, 421–423; (*b*) A. M. Dittler-Klingemann and F. E. Hahn, *Inorg. Chem.*, 1996, **35**, 1996–1999; (*c*) A. M. Dittler-Klingemann, C. Orvig, F. E. Hahn, F. Thaler, C. Hubbard, R. van Eldik, S. Schindler and I. Fábián, *Inorg. Chem.*, 1996, **35**, 7798–7803.

10 C. Ochs, F. E. Hahn and R. Frohlich, *Chem. – Eur. J.*, 2000, **6**, 2193–2199.

11 (*a*) B. A. Brennan, G. Alms, M. J. Nelson, L. T. Durney and R. G. Scarrow, *J. Am. Chem. Soc.*, 1996, **118**, 9194–9195; (*b*) R. G. Scarrow, B. S. Strickler, J. J. Ellison, S. C. Shoner, J. A. Kovacs, J. G. Cummings and M. J. Nelson, *J. Am. Chem. Soc.*, 1998, **120**, 9237–9245; (*c*) L. Heinrich, Y. Li, J. Vaissermann, G. Chottard and J.-C. Chottard, *Angew. Chem., Int. Ed. Engl.*, 1999, **38**, 3526–3528.

12 M. T. Werth, S.-F. Tang, G. Formicka, M. Zeppezauer and M. K. Johnson, *Inorg. Chem.*, 1995, **34**, 218–228.

13 (*a*) Y.-H. Chiu, G. J. Gabriel and J. W. Canary, *Inorg. Chem.*, 2005, **44**, 40–44; (*b*) G. J. Christian, A. Llobet and F. Maseras, *Inorg. Chem.*, 2010, **49**, 5977–5985.

14 H. Keypour, A. H. Jamshidi, M. Rezaeivala and L. Valencia, *Polyhedron*, 2013, **52**, 872–878.

15 M. Kalanithi, M. Rajarajan, P. Tharmaraj and C. D. Sheela, *Spectrochim. Acta, Part A*, 2012, **87**, 155–162.

16 G. A. McLachlan, G. D. Fallon, R. L. Martin and L. Spiccia, *Inorg. Chem.*, 1995, **34**, 254–261.

17 S. J. Brudenell, L. Spiccia and E. R. T. Tiekink, *Inorg. Chem.*, 1996, **35**, 1974–1979; A. B. P. Lever, *Studies in physical and theoretical chemistry 33: Inorganic electronic spectroscopy*, Elsevier, Amsterdam, 1997.

18 B. Graham, M. T. W. Hearn, P. C. Junk, C. M. Kepert, F. E. Mabbs, B. Moubaraki, K. S. Murray and L. Spiccia, *Inorg. Chem.*, 2001, **40**, 1536–1543.

19 C. Ochs, F. E. Hahn and R. Fröhlich, *Eur. J. Inorg. Chem.*, 2001, 2427–2436.

20 M. Du, Y.-M. Guo, S.-T. Chen, X.-H. Bu and J. Ribas, *Inorg. Chim. Acta*, 2003, **346**, 207–214.

21 S. Bhattacharyya, S. B. Kumar, S. K. Dutta, E. R. T. Tiekink and M. Chaudhury, *Inorg. Chem.*, 1996, **35**, 1967–1973.

22 B. Sarkar, M. S. Ray, Y.-Z. Li, Y. Song, A. Figuerola, E. Ruiz, J. Cirera, J. Cano and A. Ghosh, *Chem. – Eur. J.*, 2007, **13**, 9297–9309.

23 B. Sarkar, S. Konar, C. J. Gomez-Garcia and A. Ghosh, *Inorg. Chem.*, 2008, **47**, 11611–11619.

24 B. J. Hathaway and A. A. G. Tomlinson, *Coord. Chem. Rev.*, 1970, **5**, 1–43.

25 M. Duggan, N. Ray, B. Hathaway, G. Tomlinson, P. Brint and K. Pelin, *J. Chem. Soc., Dalton Trans.*, 1980, 1342–1348.

26 N. J. Ray, L. Hulett, R. Sheahan and B. Hathaway, *J. Chem. Soc., Dalton Trans.*, 1981, 1463–1469.

27 E. Colacio, J. M. Domínguez-Vera, M. Gazi, R. Kivekäs, J. M. Moreno and A. Pajunen, *J. Chem. Soc., Dalton Trans.*, 2000, 505–509.

28 (*a*) M. J. Scott, S. C. Lee and R. H. Holm, *Inorg. Chem.*, 1994, **33**, 4651–4662; (*b*) M. T. Gardner, G. Deinum, Y. Kim, G. T. Babcock, M. J. Scott and R. H. Holm, *Inorg. Chem.*, 1996, **35**, 6878–6884; (*c*) R. T. Conley, *Infrared Spectroscopy, Allyn & Bacon Inc.*, Boston, 1966; (*d*) K. Nakamoto, *Infrared and Raman Spectra of Inorganic and Coordination Compounds Part A and B*, 5h edn, Wiley, New York, 1997.

29 N. Mondal, D. K. Dey, S. Mitra and V. Gramlich, *Polyhedron*, 2001, **20**, 607–613.

30 A. Bottcher, H. Elias, E. Jager, H. Lanffelderora, M. Mazur, L. Mullor, H. Paulas, P. Pelikan, M. Rudolph and M. Valko, *Inorg. Chem.*, 1993, **32**, 4131–4138.

31 R. N. Patel, S. P. Rawat, M. Choudhary, V. P. Sondhiya, D. K. Patel, K. K. Shukla, D. K. Patel, Y. Singh and R. Pandey, *Inorg. Chim. Acta*, 2012, **392**, 283–291.

32 A. Kumar Sharma and R. Mukherjee, *Inorg. Chim. Acta*, 2008, **361**, 2768–2776.
33 E. V. Rybak-Akimova, A. Y. Nazarenko, L. Chen, P. W. Krieger, A. M. Herrera, V. V. Tarasov and P. D. Robinson, *Inorg. Chim. Acta*, 2001, **324**, 1–15.
34 N. J. Lundin, I. G. Hamilton and A. G. Blackman, *Polyhedron*, 2004, **23**, 97–102.
35 F. Tuna, G. I. Pascu, J. P. Sutter, M. Andruh, S. Golhen, J. Guillevic and H. Pritzkow, *Inorg. Chim. Acta*, 2003, **342**, 131–138.
36 B. Sreenivasulu, M. Vetrichelvan, F. Zhao, S. Gao and J. J. Vittal, *Eur. J. Inorg. Chem.*, 2005, 4635–4645.
37 Y. Yahsi and H. Kara, *Inorg. Chim. Acta*, 2013, **397**, 110–116.
38 L. C. Nathan, J. E. Koehne, J. M. Gilmore, K. A. Hannibal, W. E. Dewhirst and T. D. Mai, *Polyhedron*, 2003, **22**, 887–894.
39 A. W. Addison, T. N. Rao, J. Reedijk, J. van Rijn and G. C. Verschoor, *J. Chem. Soc., Dalton Trans.*, 1984, **7**, 1349–1356.
40 K. P. Maresca, G. H. Bonavia, J. W. Babich and J. Zubieta, *Inorg. Chim. Acta*, 1999, **284**, 252–257.
41 M. Li, A. Ellern and J. H. Espenson, *Inorg. Chem.*, 2005, **44**, 3690–3699.
42 J. F. Larrow and E. N. Jacobson, *J. Org. Chem.*, 1994, **59**, 1939–1942.
43 Bruker, APEX2, SAINT, SADABS and SHELXTL Bruker AXS Inc., Madison, Wisconsin, USA, 2012.
44 (*a*) G. M. Sheldrick, *Acta Crystallogr., Sect. A: Found. Crystallogr.*, 1990, **46**, 467–473; (*b*) G. M. Sheldrick, *Methods Enzymol.*, 1997, **276**, 628–641.
45 G. M. Sheldrick and T. R. Schneider, *Methods Enzymol.*, 1997, **277**, 319–343.
46 G. M. Sheldrick, *SHELXS97*, University of Gottingen, Germany, 1997.
47 Y. Zhao and D. G. Truhlar, A new local density functional for main-group thermochemistry, transition metal bonding, thermochemical kinetics, and noncovalent interactions, *J. Phys. Chem. A*, 2006, **125**, 194101.
48 M. J. Frisch, *et al.*, *Gaussian 09, Revision A.02*, Gaussian, Inc., Wallingford, CT, 2009.